

Transient Stress Analysis on Medium Modules Spur Gear by Using Mode Super Position Technique

Ali Raad Hassan

Abstract—Natural frequencies and dynamic response of a spur gear sector are investigated using a two dimensional finite element model that offers significant advantages for dynamic gear analyses. The gear teeth are analyzed for different operating speeds. A primary feature of this modeling is determination of mesh forces using a detailed contact analysis for each time step as the gears roll through the mesh. ANSYS software has been used on the proposed model to find the natural frequencies by Block Lanczos technique and displacements and dynamic stresses by transient mode super position method. The effect of rotational speed of the gear on the dynamic response of gear tooth has been studied and design limits have been discussed.

Keywords—Spur gear, Natural frequency, transient analysis, Mode super position technique.

I. INTRODUCTION

ROTATING members like shafts, pulleys, gears, etc are subjected to dynamic loads. In gears the dynamic load creates bending stresses at the tooth root which can lead to fatigue failure. One of the major concerns in the design of power transmission gears is the reduction of dynamic load. Research work has revealed that the basic mechanism of noise generated from gears is due to vibration excited by the dynamic load. The life and reliability of a gear transmission is reduced by high dynamic load. Minimizing gear dynamic load will decrease gear noise, increase efficiency, improve pitting fatigue life, and help prevent gear tooth fracture. [2], [3], [7], [9], [10], [13] and [16] worked in the area of static and dynamic analysis of spur gear tooth. In this work, three tooth segment of a 30 tooth pinion meshing with 60 tooth gear has been considered. Trochoid fillet at the base of the involute tooth is generated using rack tip.

II. GEAR TOOTH GEOMETRY

The pinion has a pitch diameter of 240mm, module of 12mm and a nominal pressure angle of 20 degree. The pinion has standard full depth teeth with addendum of 1.0 m and dedendum of 1.25 m. The face width of the pinion is 60mm. A 6425N load is considered along the line of action of the model. Development of the finite element model begins with data describing the outline of a single tooth and its fillets from

the center of the tooth space on one side to the center of the tooth space on the other side. Several different curves make up the tooth outline: concentric circular arc at the tooth tip defining the addendum circle, involutes on the two sides of the tooth, and trochoides between the involutes and the bottom lands at the base of the tooth. The tooth side involutes, fillet trochoides, and bottom lands were shaped to model a gear cut with a rack form cutter. Coordinates for the surface profile of the tooth come from a kinematic analysis of the cutting process [4]. Both the rack form cutter and the resulting gear surface are tangent to each other at the cutting points, which generate the gear shape from the rack shape. The involute is generated by points on the side of the rack form, the gear tooth fillet is generated by the tip of the rack form, and the bottom land is generated by the top surface of the rack form tooth. With the appropriate rotations, this slope and radius locates the direction and point of application of the gear mesh force on the central tooth. For this mesh, the gear parameters used are: module (m) 12mm, the pressure angle (ϕ) 20 degrees, gear ratio (i) 2, modulus of elasticity (E) 2.15×10^5 N/mm², poisson's ratio (ν) 0.3, Steel mass density (ρ) 8.75×10^{-9} N.s²/mm⁴ and the speed (n) 1440rpm.

III. NATURAL FREQUENCY CALCULATION

Fig. 1 shows the gear tooth as a cantilever beam. It is easy to calculate the natural frequency of this beam by the following equation [12]:

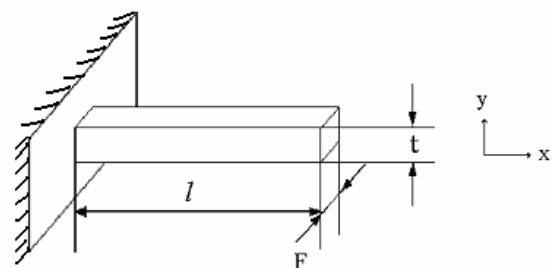


Fig. 1 Gear tooth modeled as a cantilever beam

$$\omega_n = \sqrt{\frac{k}{mass}} \quad (1)$$

k is the stiffness of the beam and it can be calculated from the following equations:

Ali Raad Hassan, PhD, Chief Engineers at Ministry of Industry and Minerals (Baghdad), Iraq (E-mail: ali_gears@yahoo.com).

$$k = \frac{3EI}{l^3} \quad (2)$$

$$I = \frac{F \cdot t^3}{12} \quad (3)$$

The length of the beam l is equal to the height of the tooth while the width of the beam t is the tooth thickness at pitch circle radius ($\pi m/2$).

$$mass = \rho(l \times t \times F) \quad (4)$$

Where, ρ is the mass density of Steel and F is the tooth face width. By using the above formula, the natural frequency is calculated using the equation (1) and is equal to 89065rad/sec.

IV. NATURAL FREQUENCY BY RAYLIEGH'S METHOD

Rayleigh's method can also be used to find the natural frequency of continuous systems. This method is much simpler than exact analysis for systems with varying distribution of mass and stiffness. Although the method is applicable to all continuous systems, it is applied to beam in this section; the natural frequency by this theory is [8]:

$$\omega_n^2 = \frac{\int_0^l EI \left(\frac{d^2 u(x)}{dx^2} \right)^2 dx}{\int_0^l \rho A (u(x))^2 dx} \quad (5)$$

The shape function $u(x)$ of cantilever beam can be taken as [12]:

$$u(x) = C_1 \left(\frac{x^5}{l^5} - \frac{5x}{l} + 4 \right) \quad (6)$$

By substituting Eq. (6) in Eq. (5) and applying the required gear details of the selected model, the resulting value of the natural frequency is (100423rad/sec).

V. STRESS CALCULATION

The load acting during the entire period of engagement is not uniform. In the beginning, at the start of engagement, two pairs of teeth will be in contact and it is assumed each pair will carry only half of the load, and the contact point will be in the tip of one of these teeth, but due to rotation, during the engagement, a new stage of contact is effected when a single pair of teeth is in contact near the pitch circle. This is called a single tooth contact and the first point of contact of this new stage is called the highest point of single tooth contact (HPSTC). Hence, loads equal to 6425N (total load) are applied to the end of the cantilever beam at an angle equal to the pressure angle of the two mating gears, namely 20 degrees. The height of the beam (l) will be assumed to be the distance between the pitch radius and root radius of the gear. The axial and radial components of this load are taken as the X-direction and Y-direction components of the load at a point corresponding to the pitch radius of the cantilever beam where the load is full value, which are 6037.5N, and 2197.4N respectively. The stresses in X and Y directions can be calculated by the following equations:

$$\sigma_x = \frac{P \sin \phi}{F \cdot t} \quad (7)$$

$$\sigma_y = \frac{P \cos \phi \times l}{\frac{F \cdot t^2}{6}} \quad (8)$$

Where, t is the thickness of the tooth at the critical section (root of the tooth), F is the face width of the tooth, P is the total load and σ_x and σ_y are the maximum stresses of the beam in X and Y axes respectively. From this formulation, the obtained value of stress in X direction for the proposed model is 1.94MPa, and the stress in Y direction is 25.488MPa respectively.

VI. FINITE ELEMENT MODEL

A model consisting of a three tooth section of a 20 tooth of 12mm module pinion was developed with the general purpose finite element software ANSYS. Figs. 2 show the finite element grid for the three tooth gear segment for this model. Successive reflections of the coordinates for the initial tooth generated segments of three equally spaced, identical teeth are noted. Both the tooth surface and the inside rim surface are unconstrained. The total angle subtended by the segment is 52 degrees. The radial lines defining the ends of the three teeth segment is at ± 26 degrees from the centre line of the model. An eight noded iso-parametric plane stress quadratic quadrilateral element was used to build the finite element model inside the frameworks described above. This element has a quadratic displacement function and is well-suited for analyzing irregular shapes. Each node in the element has two degrees of freedom - translations in the X and Y directions. The plane stress option with unit thickness was used and scaled to the actual model thickness of 60mm. To specify the boundary conditions, all the nodes on the two radial lines defining the ends of the segment and the bottom rim were selected and given zero displacement in both directions. To apply the load at a node, the grid had to have a node point at or near this loading point. Fig. 3 show the right and left sides of the central tooth of the model (tension and the compression sides), with the nodal numbers in position and stresses at these nodes will be evaluated for comparison purposes later. The complete model has 320 elements, 1071 nodes, and 2142 degrees of freedom. The backup ratio and the rim thickness in this model are 2.5 and 67.5mm respectively.

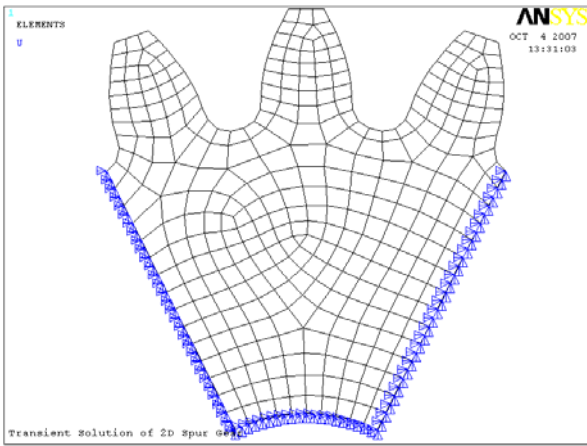


Fig. 2 Finite element mesh

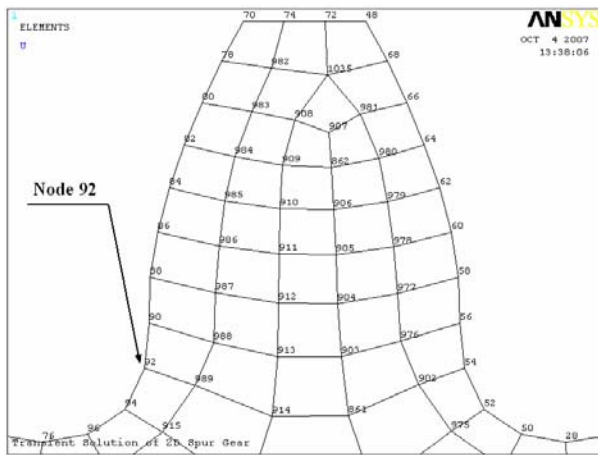


Fig. 3 Enlarged view of central tooth of the model

The plane stress option with unit thickness was used and scaled to the actual model thickness of 60mm. To specify the boundary conditions, all the nodes on the two radial lines defining the ends of the segment and the bottom rim were selected and given zero displacement in both directions. To apply the load at a node, the grid had to have a node point at or near this loading point. Fig. 3 show the right and left sides of the central tooth of the model (tension and the compression sides), with the nodal numbers in position and stresses at these nodes will be evaluated for comparison purposes later. The complete model has 326 elements, 1097 nodes, and 2194 degrees of freedom. The backup ratio and the rim thickness in this model are 2.5 and 140.625mm respectively.

VII. MODAL ANALYSIS

Having obtained the finite element model, a modal analysis has been conducted on the same. The global stiffness matrix [K] and global mass matrix [M] was obtained by assembling the element stiffness and mass matrices, respectively. The natural frequencies of the gear tooth were obtained by solving the eigen value problem given by the following equation:

$$[K]\{U\} = \omega_n^2 [M] \{U\} \quad (9)$$

where ω_n is the natural frequency of the system and $\{U\}$ is the corresponding normalized eigen vector (mode shape). The eigen values and eigen vectors were obtained using Block Lanczos method[14]. The first five natural frequencies and corresponding normalized eigen vectors were calculated using this technique. The first five natural frequencies of the gear tooth obtained for the selected model are given in Table I.

TABLE I
FIRST FIVE NATURAL FREQUENCIES

Mode	Natural frequency of the model	
	cycle/sec	rad/sec
1	14674	92199
2	15584	97917
3	15666	98432
4	22368	140542
5	26720	167886

VIII. LOAD DISTRIBUTION ON GEAR TOOTH

Load distribution on gear tooth In order to conduct a static stress analysis the loads have to be evaluated. The load on the central tooth of the finite element model, which produces the largest bending stress, is the full load acting at the highest point of single tooth contact (HPSTC). The magnitude of load at any point of contact on profile of gear tooth as the load moves from root to tip of tooth depends on the contact ratio. Fig. 4 shows the contact path, the contact ratio C_R is defined as the ratio of length of path of contact AB to base circle pitch P_b .

$$C_R = \frac{\overline{AB}}{P_b} \quad (10)$$

Where:

$$\overline{AB} = \sqrt{r_{a1}^2 - r_{b1}^2} + \sqrt{r_{a2}^2 - r_{b2}^2} - (r_{b1} + r_{b2}) \tan \phi \quad (11)$$

The contact ratio of the spur gear, for the present case is 1.63. Fig. 5 shows the magnitude of loads at various points along the path of contact. The maximum normal load P acting on the gear tooth sector of the proposed model is taken as 6425N based on the strength of gear tooth material. This normal load is considered in terms of its components in radial and tangential directions taking into account the pressure angle (Load angle γ_w) at any point under consideration, and then the tangential load and radial load can be determined by the following equations:

$$P_t = P \cos \gamma_w$$

$$P_r = P \sin \gamma_w$$

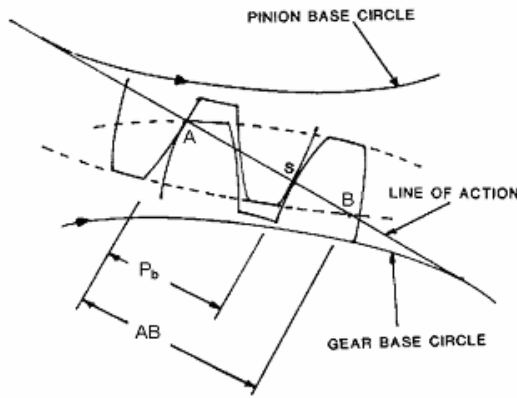


Fig. 4 Contact path

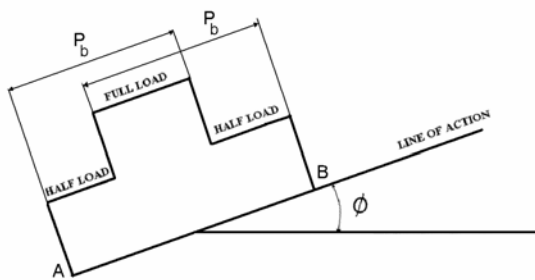


Fig. 5 Magnitude of loads along the path of contact

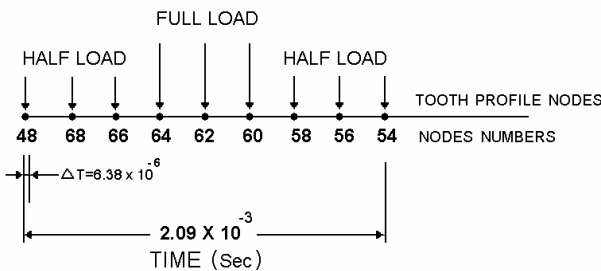


Fig. 6 Load on various nodes of the selected model

Fig. 6 show the right side (Tension side) of the profiles of the central tooth of the selected model, shown in Fig. 3, stretched out into straight line with the nodes indicated for the purpose of application of loads. The load that have been applied for the various runs of static analysis are indicated on the respective nodes starting from the extreme left end (node 48) to the final point of contact (node 54) of the model[1].

IX. STATIC BENDING STRESS ANALYSIS

After computing the natural frequencies and the mode shapes the forced response is obtained using the modal superposition technique [13]. The method is computationally efficient particularly for a large sized problem. The governing differential equation of gear tooth considering the damping is:

$$[K] \{\delta\} = [P] \tag{12}$$

The moving load during the time of contact is considered in 9 intervals. At each time interval, the position and magnitude of the load is different and shown in Table II. The static stress on all the elements for each load is obtained by using ANSYS Finite Element software and the static bending stresses on the critical nodes (Node 92) on the compression side are listed in the same table.

TABLE II
STATIC BENDING STRESS OF THE MODEL FOR EACH LOAD STEP

Load Step	Load Applied on Nodes	Load	Stress at node 92 (MPa)	
			σ_x	σ_y
1	48	Half	1.732	20.399
2	68	Half	1.534	17.863
3	66	Half	1.331	15.259
4	64	Full	2.231	24.989
5	62	Full	1.799	19.539
6	60	Full	0.694	7.236
7	58	Half	0.480	4.765
8	56	Half	0.268	2.605
9	54	Half	0.086	0.987

X. TRANSIENT ANALYSIS

After computing the natural frequencies and the mode shapes the forced response is obtained using the modal superposition technique [12], [14]. The method is computationally efficient particularly for a large sized problem. The governing differential equation of gear tooth considering the damping is:

$$[M] \{\delta''\} + [C] \{\delta'\} + [k] \{\delta\} = \{P(t)\} \tag{13}$$

Where [M], [C] and [K] are global mass, damping and stiffness matrices of size (n×n), respectively. The {P (t)} is the external time varying load of size (n×1).The symbols {δ}, {δ'}, {δ''} are the displacement, velocity, acceleration vectors of size (n×1). Eq.(13) has to be recast such that m uncoupled equations in a single degree may be obtained. The recast equation can be obtained by substituting for {δ}, as {δ} = [U] {p}, where [U] is a matrix (size n×m) of the first m eigen vectors (m<<n), and {p} is a generalized displacement vector of size (m×1). Pre multiplying Eq. (13) by [U]^T, gives:

$$[U]^T [M] [U] \{p''\} + [U]^T [C] [U] \{p'\} + [U]^T [K] [U] \{p\} = [U]^T \{P(t)\} \tag{14}$$

Here [U]^T [M] [U] is a unity diagonal matrix of size (m×m) and [U]^T [C] [U] is a diagonal matrix of size (m×m). The diagonal elements of these matrices are 2ξ_i ω_i where ξ_i are the damping ratio and ω_i are the natural frequencies for i= 1, 2, 3,m. The [U]^T [K] [U] is also a diagonal matrix with the square of the natural frequencies (ω₁², ω₂², ω₃², ..., ω_m²) as the diagonal terms. The resulting decoupled set of equations are solved as standard single degree of freedom system and the

resulting displacement vector is transformed back to represent the gear tooth displacements.

$$[U]^T [C] [U] = 2 \begin{bmatrix} \xi_1 \omega_1 & 0 & & & \\ 0 & \xi_2 \omega_2 & & & \\ & & 0 & & \\ & & & 0 & \\ & & & & \xi_m \omega_m \end{bmatrix} \quad (15)$$

In order to obtain the diagonal elements of the $[U]^T [C] [U]$ given in Eq. (15), the damping matrix is expressed as a linear combination of $[M]$ and $[K]$ (Rayleigh damping), that is:

$$[C] = \alpha [M] + \beta [K] \quad (16)$$

Where α and β are constants to be determined. Then,

$$2 \xi_1 \omega_1 = \alpha + \beta \omega_1^2, 2 \xi_2 \omega_2 = \alpha + \beta \omega_2^2, \dots, 2 \xi_m \omega_m = \alpha + \beta \omega_m^2 \quad (17)$$

From the finding of Mohammad *et al.* [6] the values for mild steel material, $\xi_1 \omega_1 = 2.0$ and $\xi_3 \omega_3 = 3.2$, where ω_1 and ω_3 are the first and third natural frequencies in rad/sec. Using these two expressions, the damping ratio for other modes are calculated by substituting in Eq. (17). Since for most industrial problems ($\omega_3 \gg \omega_1$) including the first three natural frequencies to compute the dynamic transient response is fairly accurate. After substituting the values of ω_1 and ω_3 of the model from Table I in Eq. (17), the values of α and β are obtained as 13.2 and 8×10^{-8} respectively.

A. Time Steps

The time of contact T of gear tooth depends on the rotational speed of the gear. If the gear is assumed to run at a speed of n-rpm, the time taken for one revolution of the gear will be $(60/n)$ sec. In one revolution, Z number of teeth will get engaged and disengaged.

$$\Delta T = \frac{1}{10 \omega_m} \quad (18)$$

Where Z is gear number of teeth. Then the time taken for one pair of teeth in engagement will be $(60 / n \cdot Z)$ sec, which will be (2.09×10^{-3}) sec in the selected model. The time taken for one pair of teeth in engagement can be divided into required number of steps (NTS - number of time steps). One time step ΔT can be calculated by considering the number of modes, which are expected to contribute to the dynamic response. So, the third frequency of the model is (15666 cycle/sec) which is taken from the finite element modal analysis results in Table 1; the time interval obtained is (6.38×10^{-6}) sec and is shown in Fig. 6, if the natural period of the m^{th} mode is T_m , a choice of ΔT equal to $T_m/10$ should give a reasonable dynamic response up to m^{th} mode [13]. Therefore,

$$TNTS = \frac{60}{\Delta T \cdot N \cdot Z} \quad (19)$$

Where, TNTS is the total number of time steps or intervals. So, the total number of intervals (time steps) for the model is 326 which mean that there are about 40 intervals between each two nodes shown in Fig. 6. At any time, two nodes are considered to calculate the load vector for that time interval. The actual load at a point is distributed in inverse proportion

to its distance from either node, to the two nodes under consideration as shown in Fig. 6. The Initial conditions for displacements and velocities for the gear tooth in the proposed model are taken as zero for all degrees of freedom. The third mode is selected for the mode superposition technique. At each time interval, the acting load is calculated and fed into the mode superposition part in ANSYS software and the corresponding deformation and stress are thus obtained. The dynamic displacements and dynamic stresses in the X and Y directions in the central tooth root portion of the selected gear model, which are at node 92, are plotted in condition of 1440rpm. The dynamic analysis is also carried out for the following four speeds of gear namely, 360rpm, 720rpm, 1440rpm and 1800rpm.

XI. RESULTS

Figs. 7 and 8 show the dynamic displacements in the X and Y directions of the selected model at node 92. Figs. 9 and 10 show the dynamic stresses at X and Y directions of the model at node 92. Figs. 11 and 12 show the dynamic shear stress (τ_{xy}) and dynamic von Mises stress of the model at node 92.

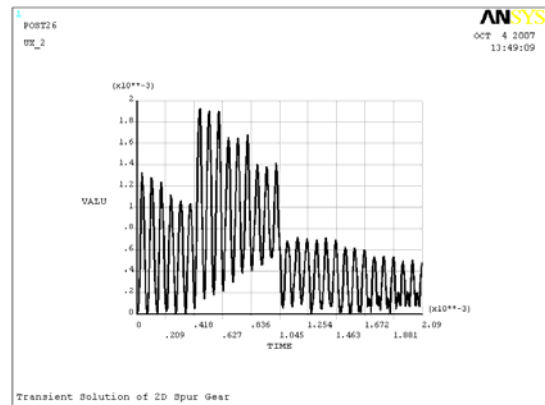


Fig. 7 Displacement of the model in X-Direction

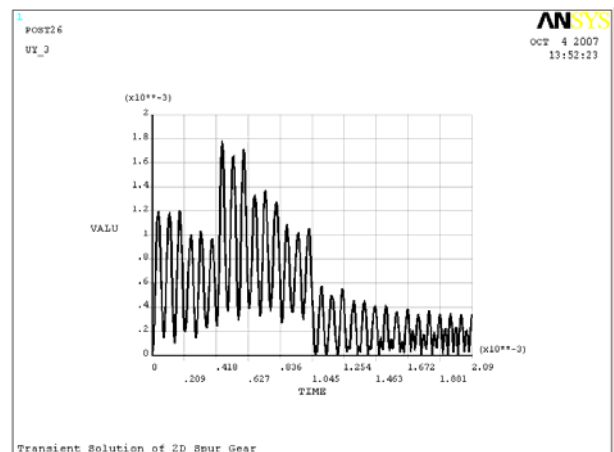


Fig. 8 Displacement of the model in Y-Direction

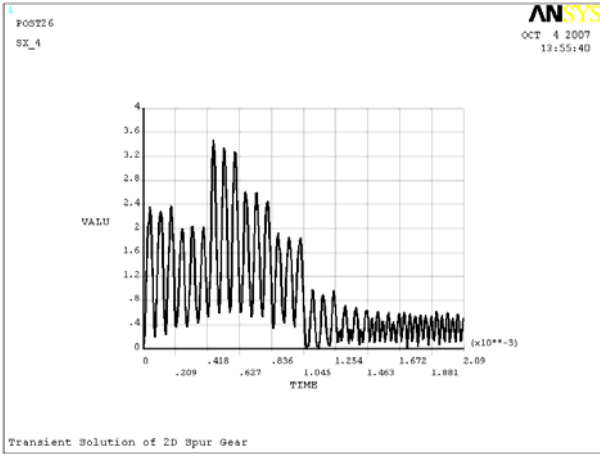


Fig. 9 Dynamic Stress of the model in X-Direction

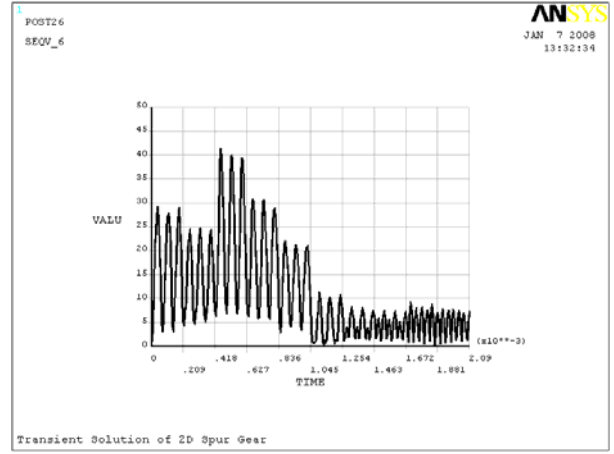


Fig. 12 Dynamic von Mises Stress of the model

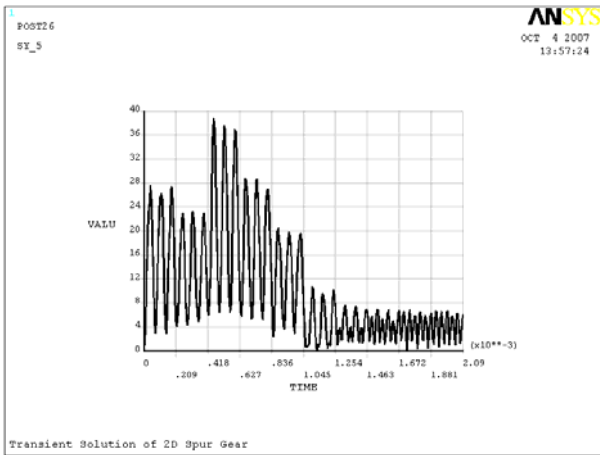


Fig. 10 Dynamic Stress of the model in Y-Direction.

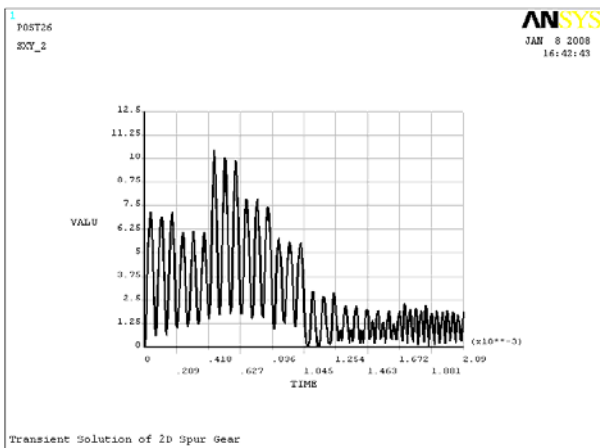


Fig. 11 Dynamic Shear Stress of the model

Table III lists the Maximum values of σ_x , σ_y , τ_{xy} and von Mises stresses of the model at node 92 for different speeds. Figs. 13, 14 and 15 show the relation curves of σ_x , σ_y and von Mises stresses with the rotational speeds, respectively.

TABLE III
MAXIMUM DYNAMIC STRESSES FOR EACH SPEED OF THE MODEL

Speed (rpm)	σ_x (MPa)	σ_y (MPa)	τ_{xy} (MPa)	von Mises (MPa)
360	2.119	20.343	5.723	21.701
720	2.623	28.127	7.51	29.867
1440	3.512	39.006	10.441	41.78
1800	3.918	44.217	12.022	47.225

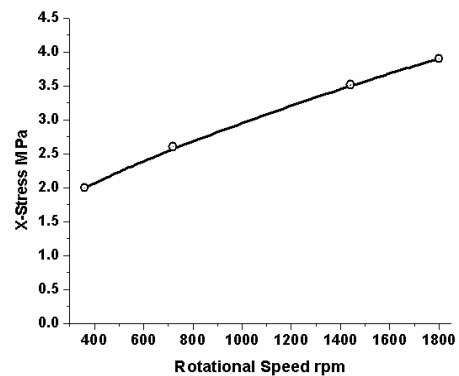


Fig. 13 Curve Relation of the Speed and Maximum Dynamic Stress in X-Direction

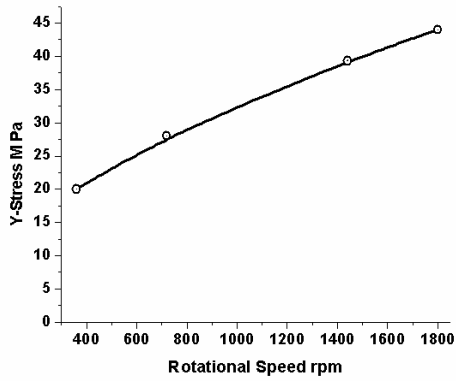


Fig. 14 Curve Relation of the Speed and Maximum Dynamic Stress in Y-Direction

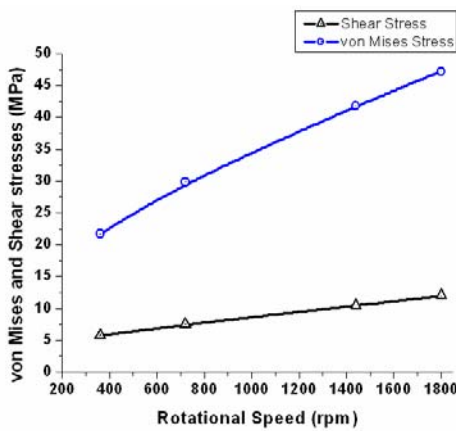


Fig. 15 Curve Relation of the Speed and Maximum Dynamic von Mises and Shear Stresses

A. Checking for Plot Fluctuation

The correctness of the results in Figs. 7 to 12 were verified by the following procedure, the number of peaks for a selected time period was calculated for each of the above plots. The frequency of the response, in cycles per seconds, can be calculated by dividing the number of peaks for a selected time period by the time taken for the same. For example; at Fig. 10 (which shows the dynamic stress of the model in Y-direction) for time period (0 to 0.418×10^{-3} sec) the number of peaks was 6, so; the resulting frequency was calculated by dividing 3 on 0.417×10^{-3} sec, which yields (14354 cycle/sec). It was clear that this value matches with fundamental natural frequency of the model (first natural frequency of the model in Table I).

XII. DISCUSSION

The natural frequency of the tooth obtained by Rayleigh's method (Eq. 5) was 100423rad/sec. The natural frequency obtained by beam formulation (Eq.1) was 89065rad/sec. It was noted in Rayleigh's method that the assumed shape $u(x)$ unintentionally introduces a constraint on the system (which amounts to adding additional stiffness to the system), and hence the frequency given by Eq. (5) is higher than the exact

value. The natural frequency obtained from Eq. (1) is more reasonable and recommended. The first natural frequency obtained from finite element modal analysis was 92199rad/sec; there is a good agreement between this value and the recommended natural frequency value obtained from Eq. (1). It was observed from the plots (shown in Figs. 9 and 10) that the dynamic stresses were varied with a time period of 6.96×10^{-5} sec whereas the time period of the fundamental natural frequency was 6.814×10^{-5} sec. So, the dynamic stresses are varying periodically with fundamental bending vibration time period of the model. The dynamic stress plots at tooth root where (shown in Figs. 9 and 10) and deformation at the tooth root were (shown in Figs. 7 and 8), three important distinguishable regions were observed. In the first region of the displacements and dynamic stresses during starting of engagement of the gear tooth were zero, and both the pairs of teeth were contact and share normal load equally. In the second region, displacements and dynamic stresses were high compared to all other regions, in this region, a single pair of gear tooth will be in contact and full load act on the gear pair under study. In the third region again, two pairs of gear teeth were in contact and share load equally. From the dynamic analysis results, the dynamic stresses at the root are lesser when the load was at the tip, and were high when the load was at the mid height [that is at HSPTC- the highest point of single tooth contact] at this point the full load was acting. From the static analysis, the maximum values of σ_x and σ_y were at node 92 of the model lie in the root at left side (compression side) of the central tooth. For the actual load distribution on the gear profile obtained by finite element method the stresses σ_x and σ_y were 2.231MPa and 24.989MPa, respectively, when full load is at HSPTC point (node 64). By beam gear design approach the values of σ_x and σ_y calculated from Eqs.7 and 8 were 1.94MPa and 25.488MPa, respectively, this shows good agreement between these values if the differences between the tooth and beam shapes are considered. From the dynamic stress analysis stress plots at the root of the model (node 92; the maximum σ_x , σ_y , τ_{xy} and von Mises stress were 3.512MPa, 39.296MPa, 10.441MPa and 41.78MPa respectively. Referring to Figs. 9 and 10, it was observed that the magnitude of static stresses (σ_x and σ_y) at the point of application was half of the enveloping curves of the dynamic stresses (mean of the maximum and minimum dynamic stresses). The amplitude of the dynamic stress goes on increasing as the speed increases with its major frequency of variation corresponding to the fundamental frequency of the gear tooth. This may be observed from Fig. 16. It is observed from Table III that the maximum magnitudes of σ_x , σ_y , τ_{xy} , and von Mises stress at the tooth root for various speeds of the selected gear model (in the range of 360rpm to 1800rpm) were increasing gradually from 2.119MPa to 3.918MPa, from 20.343MPa to 44.217MPa, from 5.723MPa to 12.022MPa and from 21.711MPa to 47.225MPa respectively, for increase in speed from 360rpm to 1800rpm. The variation is shown in Figs. 13, 14 and 15. Therefore, the dynamic stresses at the root of the low modules spur gear tooth were increasing with increase in the rotational speed of the gear.

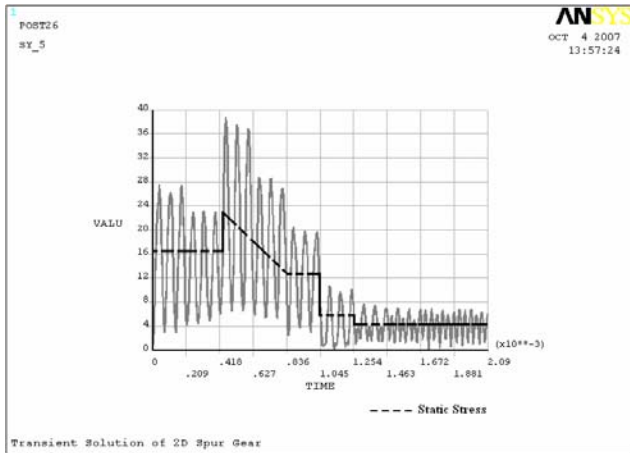


Fig. 16 Stress response of the 1st model in Y-Direction

A. Food for Thought

Modal super position technique assumes that any transient disturbance of member was the sums total of the disturbances due to the first few modes of vibration. In reality the contribution from the higher modes die down very fast in comparison with the 1st mode. This has been experimentally observed to be true. This is the basis of subsections 7 to 9 of this paper.

Referring to section 14.8 (Dynamic Factor) of [15], dynamic stress is obtained by multiplying by the Lewis form factor c_v (Equation 14.27):

- (i). This factor does not take into account gear face width (F).
- (ii). It is assumed that the static stress is multiplied by a factor involving peripheral velocity of the gear[5].
- (iii). It is well known that when the face width is increased the gear tooth becomes stronger and, hence the magnitude of dynamic stress is smaller than the gear with smaller face width, but this has not been taken into account in this formula.
- (iv). During the transient phase the gear tooth is expected to vibrate in one or more of its natural frequencies, which has not been assimilated or taken into account in the existing code.

In the present approach these aspects have been taken into account.

XIII. CONCLUSION

Modal super position technique assumes that any transient disturbance of member is the sum totals of the disturbance due to the first few modes of vibration. In reality the contribution from the higher modes die down very fast in comparison with the first mode. This has been experimentally observed to be true. It is found that as the rotational speed of gear increases, the bending stress of dynamic stress also increases. For the moving load, the ratio of maximum dynamic bending root stress to maximum static bending root stress is increases.

REFERENCES

- [1] Ali Raad Hassan, Thanigaiyarasu G. and Ramamurti V. (2008). 'Effects of Natural Frequency and Rotational Speed on Dynamic Stress in Spur Gear', Proceeding of World Academy of Science, Engineering and Technology, Volume 36, pp. 1279-1287.
- [2] ANSI/AGMA (2001-B88) (1988). 'Fundamental Rating Factors and Calculation Methods for Involute Spur and Helical Gear Teeth', American Gear Manufacturers Association, Arlington, VA.
- [3] Eiff von H., Hirschmann K.H., Lechner G. (1990). 'Influence of gear tooth geometry on tooth stress of external and internal gears', ASME Journal of Mechanical Design 112 (4) 575-583.
- [4] Hefeng B., Savage M., Knott R.J. (1985). 'Computer modeling of rack generated spur gears'. Mechanism and Machine Theory 20 (4) 351-360.
- [5] Khurmi R.S., Gupta J.K. (2006). 'A Textbook of Machine Design', Eurasia Publishing House (PVT.) LTD., New Delhi, pp 1035-1038.
- [6] Mohammad D., Khan N U, Ramamurti V. (1995). 'On the role of Rayleigh damping'. Journal of Sound and Vibration 185 (2) 207.
- [7] Oda S., Nagamura K., Aoki K. (1981). 'Stress analysis by thin rim spur gears by finite element method'. Bulletin of the Japanese Society of Mechanical Engineers 24 (193) 1273-1280.
- [8] Rao Singiresu S. (2004). 'Mechanical Vibrations' 4th Edition, Pearson Education (Singapore) Pte. Ltd., India Branch, Delhi.
- [9] Ramamurti V., Reddy K. R. K. (2001). 'Dynamic analysis of spur gear tooth'. The Institution of Engineering (India) Journal 82 33-40.
- [10] Ramamurti V., Gupta L. S. (1979). 'Dynamic stress analysis on spur gear teeth'. ASME Conference 38, DET.
- [11] Ramamurti V., Vijayendra Nayak H., Sujatha C. (1998). 'Static and dynamic analysis of spur and bevel gears using FEM', Mechanism and Machine Theory 33 (8) 1177-1193.
- [12] Ramamurti V. (2002). 'Mechanical Vibration Practice with Basic Theory', Narosa Publishing House, New Delhi.
- [13] Ramamurti V. (1998). 'Computer Aided Design in Mechanical Engineering', McGraw Hill Publishing Co., New York.
- [14] Seshu P. (2004). 'Text Book of Finite Element Analysis', Prentice-Hall of India, New Delhi.
- [15] Shigley J.E. and Charles R.M. (2003). 'Mechanical Engineering Design', Tata McGraw-Hill, New Delhi, 6th edition.
- [16] Wilcox L., Coleman W. (1973). 'Application of finite elements to the analysis of gear tooth stresses'. Journal of Engineering for Industry 95 (4) 1139-1148.



Ali Raad Hassan, Assistant Professor of Technical Institutes (Iraq), Chief Engineers at Ministry of Industry and Minerals (Baghdad), Iraq. He has been awarded 5 times for his researches and developments on gear manufacturing machines. Currently he got his PhD in mechanical engineering from Department of Mechanical Engineering, Anna University (India). He has more than 10 years experience in Industry.